Journal of Molecular Catalysis B: Enzymatic 69 (2011) 168–175

Contents lists available at ScienceDirect

Journal of Molecular Catalysis B: Enzymatic

journal homepage: www.elsevier.com/locate/molcatb

Amperometric electrode for determination of urea using electrodeposited rhodium and immobilized urease

Yana Velichkova[a], Yavor Ivanov[a], Ivaylo Marinov[a], Rajendran Ramesh[b], Numbi Ramudu Kamini[b], Nina Dimcheva[c], Elena Horozova[c], Tzonka Godjevargova[a,*]

[a] Department of Biotechnology, University "Prof. A. Zlatarov", Bourgas 8010, Bulgaria
[b] Department of Biotechnology, Central Leather Research Institute, Council of Scientific and Industrial Research, Adyar, Chennai 600 020, India
[c] Department of Physical Chemistry, University of Plovdiv, Plovdiv 4000, Bulgaria

ARTICLE INFO

Article history:
Received 27 September 2010
Received in revised form 20 January 2011
Accepted 27 January 2011
Available online 2 February 2011

Keywords:
Urea sensing
Urease
Amperometric sensor
Electrodeposition
Rhodium
Polymer membrane

ABSTRACT

An amperometric biosensor was developed for determination of urea using electrodeposited rhodium on a polymer membrane and immobilized urease. The urease catalyzes the hydrolysis of urea to NH_4^+ and HCO_3^- ions and the liberated ammonia is catalytically and electrochemically oxidized by rhodium present in the rhodinized membrane on the Pt working electrode. Three types of rhodinized polymer membranes were prepared by varying the number of electrodeposition cycles: membrane 1 with 10 deposition cycles, membrane 2 with 40 cycles and membrane 3 with 60 cycles. The morphologies of the rhodinized membranes were investigated by scanning electron microscopy and the results showed that the deposition of rhodium was like flowers with cornices-like centers. The influence of the amount of electrodeposited rhodium over the electrode sensitivity to different concentrations of ammonia was examined initially based on the cyclic voltammetric curves using the three rhodium modified electrodes. The obtained results convincingly show that electrode with rhodinized membrane 1, which contain the lowest amount of electrodeposited rhodium is the most active and sensitive regarding ammonia. It was found that the anodic oxidation peak of ammonia to nitrogen occurs at 0.60 V. In order to study the performance of urease amperometric sensor for the determination of urea, experiments at constant potential (0.60 V) were performed. The current–time experiments were carried out with urease rhodinized membrane 1 (10 cycles). The amperometric response increased linearly up to 1.75 mM urea. The detection limit was 0.05 mM. The urea biosensor exhibited a high sensitivity of 1.85 μA mM^{-1} cm^{-2} with a response time 15 s. The Michaelis–Menten constant K_m for the urea biosensor was calculated to be 6.5 mM, indicating that the immobilized enzyme featured a high affinity to urea. The urea sensor showed a good reproducibility and stability. Both components rhodium and urease contribute to the decreasing of the production cost of biosensor by avoiding the use of a second enzyme.

1. Introduction

Urea, an end product of nitrogen metabolism has great significance in clinical chemistry where blood urea nitrogen is an important indicator of possible kidney malfunction [1,2]. In medical application, urea is mainly analyzed in blood and urine. Apart from being crucial as an indicator of liver and kidney function, the blood urea test is also used as a marker for quantification and monitoring of haemodialysis treatment. Moreover, urea is widely distributed in nature and its analysis is necessary in food chemistry and environmental monitoring [3]. In food analysis, urea is routinely quantified for instance in cow's milk and in alcoholic beverages [4]. Urea can stress the environment in different ways because it acts as a nitrogenous fertilizer. It decomposes to ammonia, which is very toxic, and so it can pollute streams and rivers into which it drains [5]. Since urea is widely distributed in nature and toxic above certain concentrations, it is of utmost interest to develop cost-effective techniques for real-time monitoring in all human-related environments [6]. The conventional analytical techniques used, although precise, are time consuming and mostly laboratory bound, whereas the biosensors have the advantages of ease of use, portability and the ability to furnish real-time signals.

Most of the existing urea biosensors utilize urease as the sensing element. The urease catalyzes the hydrolysis of urea to carbonic acid and ammonia as final products [7]. Krajewska offers a review of reports on immobilizations of ureases covering the last two decades. It surveys the immobilization techniques and supportmaterials applied, in addition to the resulting properties

* Corresponding author. Tel.: +359 56 858 353; fax: +359 56 858 220.
E-mail address: godjevargova@yahoo.com (T. Godjevargova).

1381-1177/$ – see front matter © 2011 Elsevier B.V. All rights reserved.
doi:10.1016/j.molcatb.2011.01.015

of the enzymes [4]. Many matrices (e.g., polymers, sol–gels, conducting polymers, Langmuir–Blodgett films, nanomaterials and self-assembled monolayers (SAMs)) have been used to (i) provide support; (ii) impart stability to biomolecules towards variations in temperature, pH and ionic strength; (iii) increase shelf-life; and (iv) reduce cost for the fabrication of a urea biosensor [7]. Recently, composite materials based on conducting polymers, redox mediators, metal nanoparticles, nanocomposites and nanoclusters have been used to combine properties of the individual components with a synergistic performance in biosensor fabrication [8]. However, efforts are being made to fabricate a cost-effective urea biosensor with improved sensitivity and stability.

The concentration of urea is measured by monitoring the liberated ions using different types of transducers such as amperometric, potentiometric, optical, thermal, or piezoelectric [6,9–15]. Despite the great variety of transducers, the urease-based amperometric urea biosensor is considered the most promising approach, because it offers fast, simple, and low-cost detection. The response time of such a biosensor is directly associated with the hydrolysis rate of urea on the electrode surface; therefore, rapid production of NH_4^+ ions on the electrode will lead to a highly sensitive biosensor. The NH_4^+ ions are not electroactive and they are oxidized to nitrogen molecule employing two approaches – using a second enzyme or a catalytically active metal. Rodriguez et al. [16] have developed amperometric sensor for urea using two enzymes – urease and isocitrate dehydrogenase. Some researchers have developed amperometric routes by oxidation of ammonia using enzymes like glutamate dehydrogenase [17]. Other authors reported the application of catalytically active metals for ammonia oxidation. Grosman and Loffler [18] observed that rhodium has a very high catalytic activity in oxidizing ammonia into nitrogen. Similar results were reported by Cooper [19] as well. Lopez de Mishima et al. [20] developed chemical amperometric sensors based on platinum–iridium electrodeposits on platinum electrode for the determination of ammonia. The main disadvantages of these chemical electrodes are the saturation and fast poisoning of the metal catalytic surface at repeated measuring.

Based on the second approach, an amperometric measuring system has been developed so that to omit the use of a second enzyme. The biosensing element urease was immobilized on the surface of a modified polymer membrane with electrodeposited rhodium, which in turn was attached to a platinum working electrode. The enzymatically produced ammonia was catalytically and electrochemically oxidized by rhodium present in the membrane. Both components rhodium and urease contribute to the decreasing of the production cost of biosensor by avoiding the use of a second enzyme.

2. Materials and methods

2.1. Reagents

Acrylonitrile-methylmethacrylate-sodium vinylsulfonate copolymer membranes (AN copolymer) were prepared without support (cut-off 60,000 Da) as described in [21]. The ternary copolymer (acrylonitrile – 91.3%; methylmethacrylate – 7.3%, sodium vinylsulfonate – 1.4%) was a product of Lukoil Neftochim, Burgas. Tris buffer solution (pH 8.1) and other reagents were of analytical reagent grade. All solutions were prepared with double distilled water. The enzyme, Jack bean urease (EC 3.5.1.5, 270 U/mg, 545 kDa) was purchased from Merck, Germany.

2.2. Apparatus

All electrochemical measurements were performed on a PalmSens Electrochemical Instrument (Palm Instruments BV, The Netherlands) with a conventional three-electrode system comprising a platinum wire as a counter electrode, Ag/AgCl reference electrode and a platinum working electrode.

2.3. Preparation and chemical modification of PAN membranes

18 g of AN copolymer was dissolved in 100 g dimethylformamide along with 1 g lithium nitrate and 3 g glycerin until a homogeneous solution was obtained. Membranes were cast from this solution by the phase-inversion method. Distilled water with room temperature was used as a coagulating agent. A piece of the prepared PAN membranes (d = 2.4 cm) was immersed in 10% NaOH for 20 min at 40 °C. The membrane unit was then washed with distilled water and placed in 1 M HCl at room temperature for 120 min. The color of the hydrolyzed yellowish red PAN membrane turned into white. Then the modified PAN membrane was immersed in 10% solution of ethylene-diamine for 1 h at room temperature in order to react with the carboxyl groups.

2.4. Electrodeposition of rhodium on PAN membranes

Rhodium deposition was performed by cyclic voltammetry in the potential range from −0.8 to +0.2 V vs. Ag/AgCl at the scan rate of 0.01 V/s, in 2% solution containing $RhCl_3{\cdot}3H_2O$ dissolved with 0.1 N HCl, at 30 °C. A polymer membrane (d = 1 cm) was attached to the platinum working electrode by a plastic ring. The membrane was in contact with the platinum electrode surface by the non-selective side (see Fig. 1). The amount of rhodium deposited on the polymer membrane was controlled by varying the number of deposition cycles (10, 40 and 60 cycles).

2.5. Cyclic voltammetric measurements with rhodinized membrane electrodes using ammonia solution

Each rhodium membrane was attached to a platinum working electrode, using a plastic ring, with the rhodium film of the membranes facing the platinum surface of the electrode, which was then placed in an electrochemical cell containing 15 mL of Tris–HCl buffer solution (pH 8.1) under stirring at 20 °C. Cyclic voltammetry experiments were performed at potential from −0.2 to 1 V, at a scan rate of 0.01 V/s. Then 100 μL of ammonia solutions with concentrations 1 mM, 3 mM and 5 mM were separately added to the cell and the resulting current was recorded.

2.6. Immobilization of urease on rhodinized PAN membranes

Urease immobilization was carried out by incubating a rhodinized PAN membrane (d = 1 cm) in a mixture containing 500 μL of 0.1% urease (pH 6), 100 μL of 1% albumin and 50 μL of 1% glutaraldehyde solution for 24 h at 4 °C. After this period the enzyme membrane was washed with distilled water and phosphate buffer solution (pH 6) and kept at 4 °C in a buffer solution (pH 6). Albumin was added to the immobilization mixture in order to increase the hydrophilicity of the membrane carrier thus contributing beneficially to the preservation of the immobilized urease activity.

2.7. Electrochemical measurements with urease biosensor

Each urease–rhodium membrane was attached to a platinum working electrode, using a plastic ring. Chrono-amperometric measurements at constant potential were employed. A potential of 0.60 V was applied to the working electrode and the electrochemical current was awaited to become stationary. Then a series of 100 μL from a 100 mM urea solution were added to the cell and the resulting current was recorded.

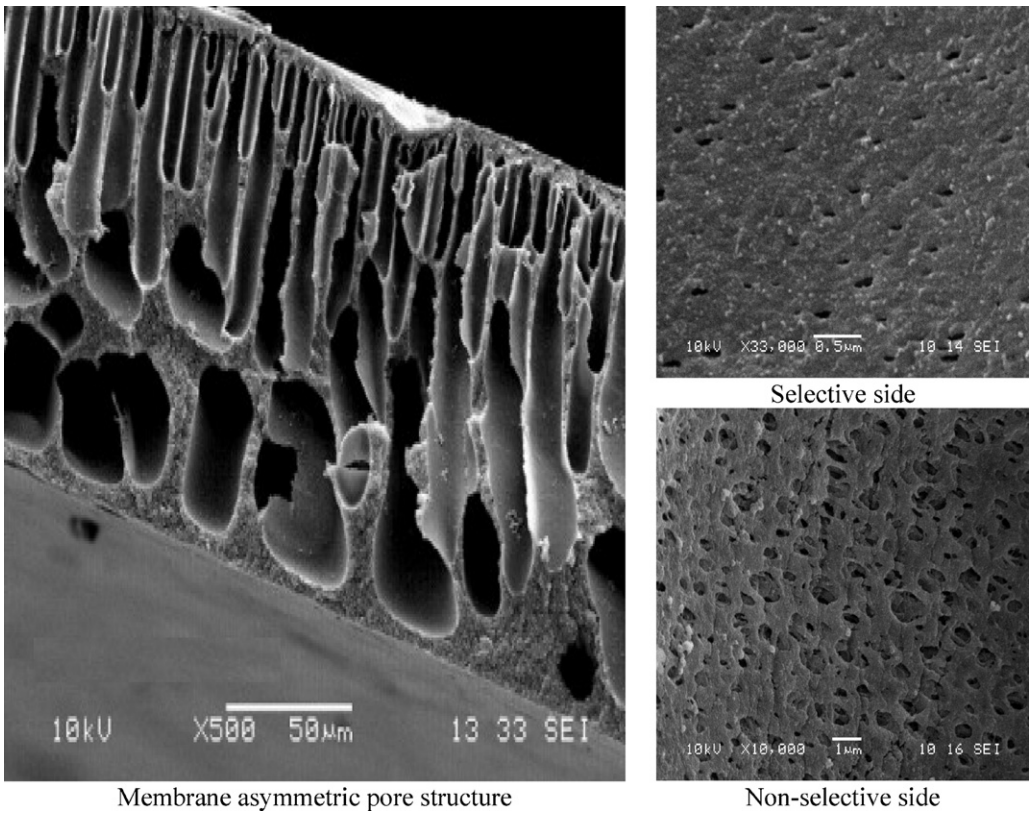

Fig. 1. SEM images of a cross-section of a membrane and its selective and non-selective sides.

2.8. SEM

The morphology of the rhodinized membranes has been investigated by scanning electron microscopy (SEM) using a JEOL JSM-6700F microscope (Japan).

3. Results and discussion

3.1. Morphology of rhodinized PAN membranes

The basic proprieties of the initial PAN membranes were investigated: membrane thickness – 150 μm, porosity volume – 81%, water flow – 0.3 $m^3\,m^{-2}\,h^{-1}$, water content – 75%. A SEM view of the cross-section of a PAN membrane (Fig. 1) clearly displays the asymmetric pore structure of the membrane. Electrochemical deposition of rhodium on three PAN membranes was employed in order to introduce different amounts of rhodium: membrane 1 with 10 deposition cycles, membrane 2 with 40 deposition cycles and membrane 3 with 60 deposition cycles. Each membrane was chemically modified in advance as described in Section 2.3. The aim of this modification was to increase the membrane hydrophilicity and their permeability in order to shorten the biosensor response time. With the increase of the number of deposition cycles a considerable increase of the rhodium amount was noticed. The thickest rhodium film was obtained after 60 deposition cycles.

The morphology of the rhodinized membranes has been investigated by scanning electron microscopy and their images are shown in Figs. 2–4. As can be seen from the figures the rhodium deposits were well dispersed on the membrane surface providing good space proximity between the metallic catalytic centers and the immobilized urease molecules. The densities of the rhodium deposits and their surface area are of a crucial importance since they define the available immobilization area as well as the swiftness of the biosensor response. More rhodium deposits with large surfaces mean, on one hand, less immobilization area, and on the other – larger sensor surface and quicker biosensor response and vice versa. Clearly, the morphology and topology of the formed rhodium clusters should depend mostly on the amount of the deposited rhodium, given that the deposition time and potential are constant. In order to investigate this dependency three modified PAN membranes were rhodinized applying different numbers of deposition cycles.

The obtained SEM images clearly revealed the distinctive features of the topography of the rhodium deposits on the PAN membranes, based on the number of cycles used for their preparation. It was observed that with the increase of the number of cycles, the amount of deposited rhodium also increased resulting in a generation of specific island-like formations with highly developed circumferences (Figs. 3 and 4). This should allow enzyme molecules to be immobilized in a very close proximity to the centers of those rhodium deposits providing a significant increase in the effectiveness of the biosensor towards urea detection.

3.2. Effect of the amount of electrodeposited rhodium on the electrochemical behavior of the amperometric ammonia sensors

Each of the membranes, mentioned above (1, 2 and 3) was used for the construction of an amperometric sensor first for detection of ammonia by attaching the membranes to a working platinum electrode (thus obtaining sensors 1, 2 and 3). Cyclic voltammetry (CV) was employed in order to establish the optimum amount of electrodeposited rhodium and the working potential of the prepared amperometric sensors, using ammonia solutions with different concentrations. The cyclic voltammograms illustrated in Fig. 5 were obtained with the three sensors (sensor 1–10 electrodeposition cycles, sensor 2–40 cycles and sensor 3–60 cycles) in a buffer solution (Tris–HCl buffer solution, pH 8.1). As can be seen from it,

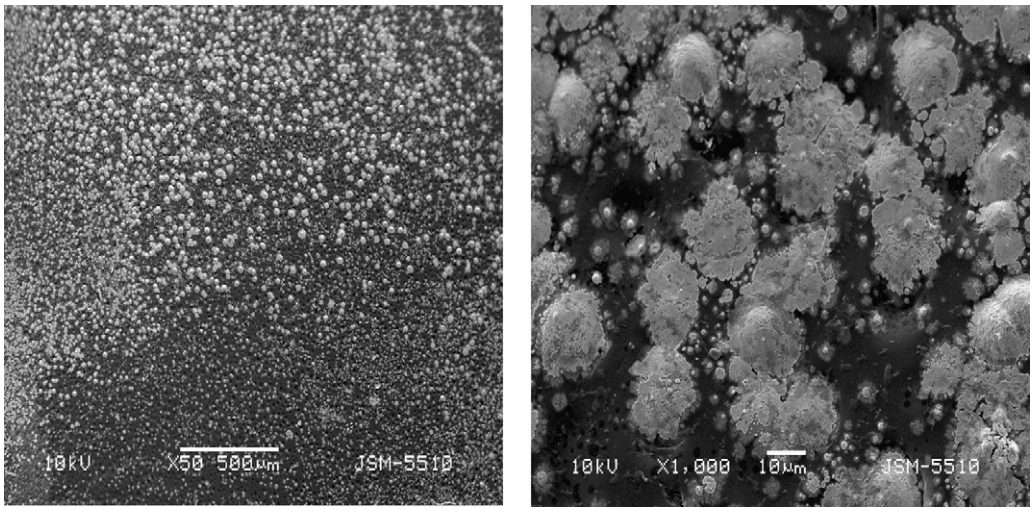

Fig. 2. SEM images of the rhodium deposited membrane 1 with 10 cycles at different magnifications.

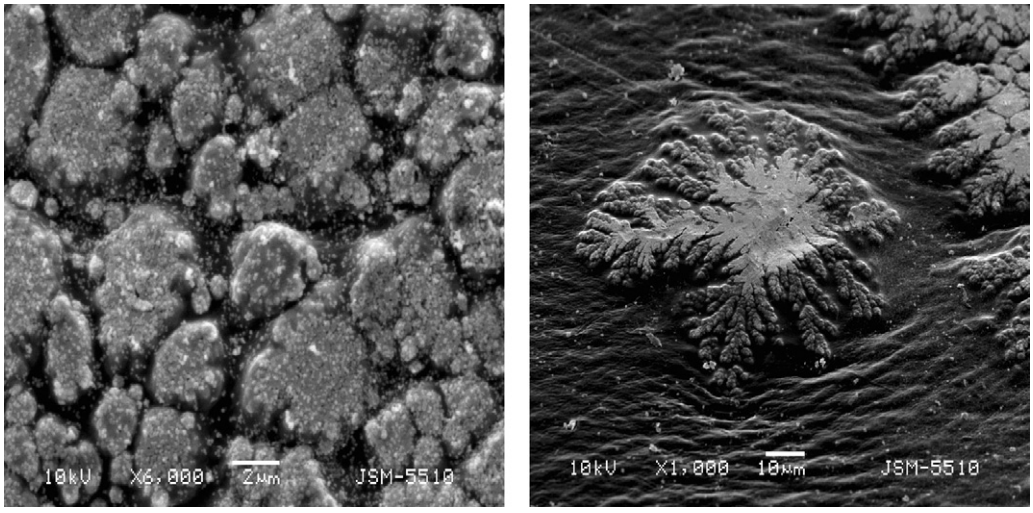

Fig. 3. SEM images of the rhodium deposited membrane 2 with 40 cycles at different magnifications.

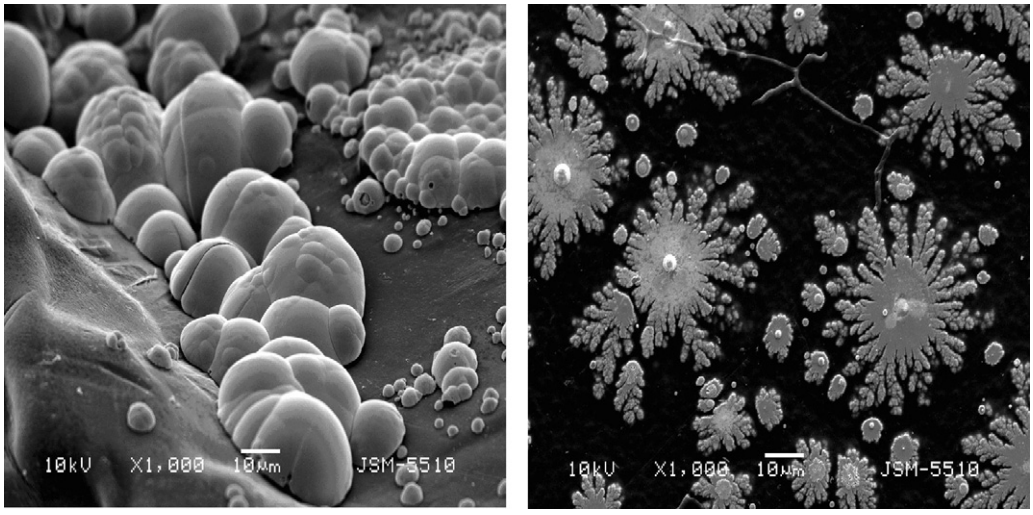

Fig. 4. SEM images of the rhodium deposited membrane 3 with 60 cycles at different magnifications.

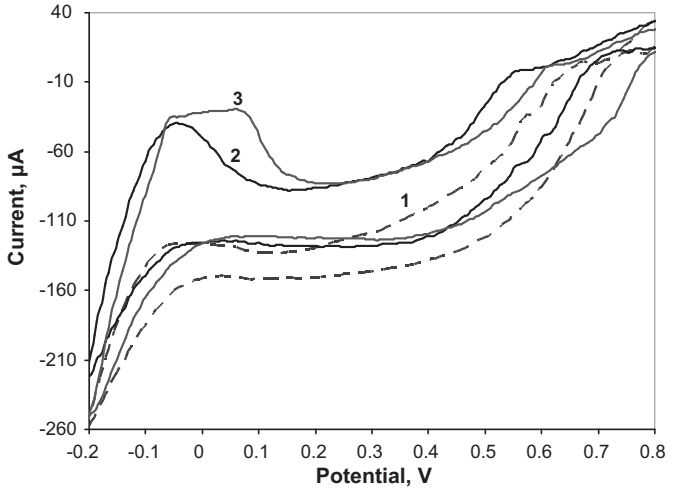

Fig. 5. CV curves of the three sensors in the presence of a Tris–HCl buffer, pH 8.1 (without ammonia).

two anodic peaks appeared on the three curves at the potentials −0.05 V and 0.60 V, respectively. The first anodic peak corresponds to oxygen adsorption on the rhodium surface and the second anodic oxidation peak – to the formation of rhodium oxide. There were no peaks corresponding to the adsorption and desorption of hydrogen on rhodium. The increase of the rhodium amount from sensor 1 to 3 resulted in increasing of the first peak maximum, as well as in shifting of the first peak potential from −0.05 to 0 V. The increase of the rhodium quantity affected the second anodic peak potential as well by shifting it from 0.60 to 0.55 V. Obviously, the greater amount of rhodium leads to wider cyclic voltammetric curves (see curve 3). This could be explained with the augmentation of the working electrode electroactive surface, being in very close proximity to the rhodinized membrane.

CV was employed to study the behavior of the three sensors in ammonia solutions with different concentrations. The CV curves of sensor 1 are presented in Fig. 6. Curve 1 represents the cyclic voltammogram of sensor 1 in a buffer solution (in the absence of ammonia). The other three curves (2, 3 and 4) depicted the CV behavior of sensor 1 in a buffer solution in which were added consecutively 100 μL of 1 mM, 3 mM and 5 mM NH_3 solutions. A noticeable increase of the amperometric current was observed after potential of 0.55 V (curves 2 and 3), while in curve 4 a prominent anodic oxidation peak was observed at 0.60 V and cathodic reduction peak at potential of 0.55 V. These results show that the oxidation peak of ammonia to nitrogen occurs at 0.60 V and similar results were also reported by other authors [22–24]. An ammonia molecule is oxidized mainly to nitrogen under alkaline conditions through a direct oxidation reaction accompanying its adsorption at the electrode; oxygen evolution rarely occurs [19,20,23].

$$NH_3 + 3OH^- = (1/2)N_2 + 3H_2O + 3e^-$$

Wasmus et al. [24] investigated the electro-oxidation and reduction of nitrogen compounds in alkaline solutions at Pt-black electrodes using a combination of cyclic voltammetry with on-line mass spectroscopic analysis of volatile products. The authors reported that ammonia could be oxidized to nitrogen at 0.60 V while oxidation to nitrogen oxides proceeded only at potentials above 0.75 V.

The CV curves of sensor 2 were presented in Fig. 7. The curve 2 obtained by adding 100 μL of 1 mM ammonia solution was identical with the initial curve 1 (without ammonia). There was a slight change in the CV curve 3 after adding 100 μL of 3 mM and a major change in the curve 4 with the addition of 5 mM ammonia solution. The observations showed that the initial peak at potential of 0 V diminished with the increase of the ammonia concentration and the amperometric current increased above a potential of 0.55 V. This means that the greater decrease of the current at 0 V and the slight increase of the current at 0.60 V could be due to the decrease in oxygen adsorption on rhodium with simultaneously occurring oxidation of ammonia. The obtained results convincingly showed that the working potential value to be selected was 0.60 V and that sensor 2 was less electroactive than sensor 1.

Almost the same pattern as for sensor 2 was observed for sensor 3 (Fig. 8). This sensor featured the membrane with the greatest amount of rhodium, which was reflected by the higher and wider initial peak at potential of 0 V. This peak gradually disappeared with the increase of the ammonia concentration. A slight increase of the current was observed at potential of 0.60 V. The obtained results with sensor 3 showed that the latter was less electroactive than sensor 1.

The CV curves of the sensors from Figs. 6–8 were compared. The observations showed that the CV curve of sensor 1 was mostly influenced by the addition of different ammonia concentrations. For the other two sensors 2 and 3, a considerable change in their CV curves was hardly observed even at the addition of 100 μL 5 mM ammonia solution. The obtained results convincingly showed that sensor 1 (with membrane 1) was the most active and sensitive regarding lower ammonia concentrations. It was also noticed that the signal-to-noise ratio increased with the introduction of a greater amount of rhodium, which was an undesirable side-effect. Taking into consideration both sensitivity and signal-to-noise ration, membrane 1 was selected for further investigations.

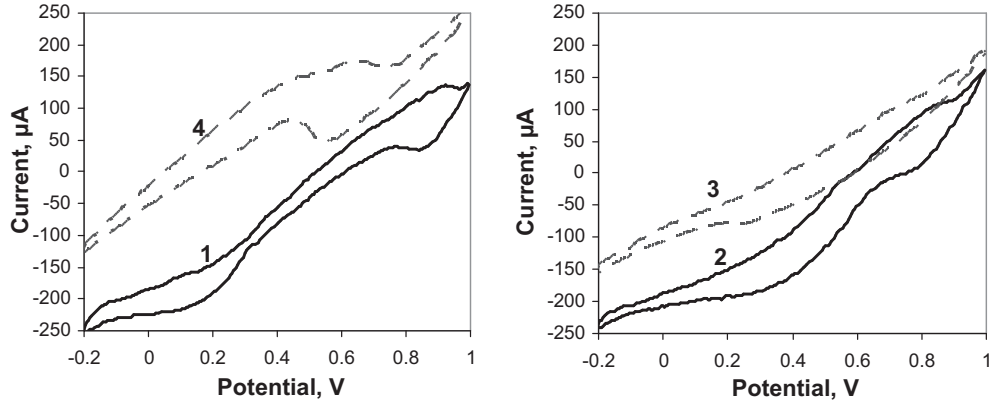

Fig. 6. CV curves of the rhodinized electrode 1 in the absence of ammonia (1) and in the presence of different concentrations of ammonia – 1 mM NH_3 (2), 3 mM NH_3 (3) and 5 mM NH_3 (4).

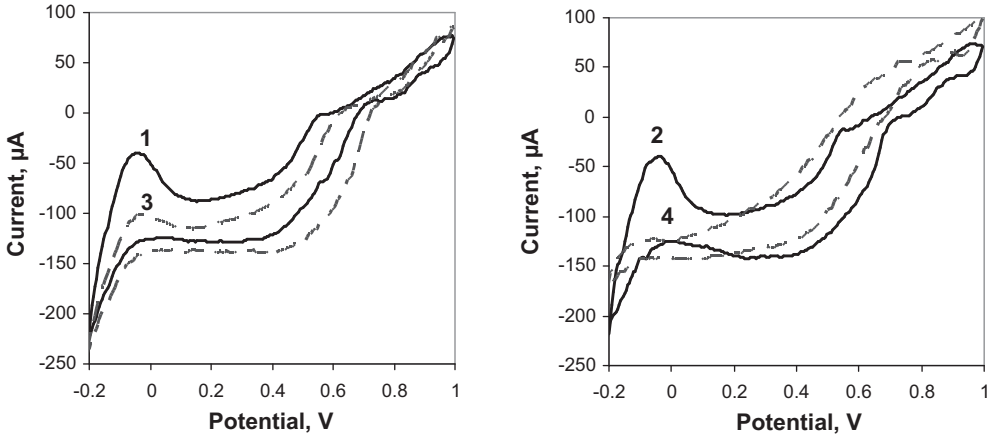

Fig. 7. CV curves of the rhodinized electrode 2 in the absence of ammonia (1) and in the presence of different concentrations of ammonia – 1 mM NH_3 (2), 3 mM NH_3 (3), and 5 mM NH_3 (4).

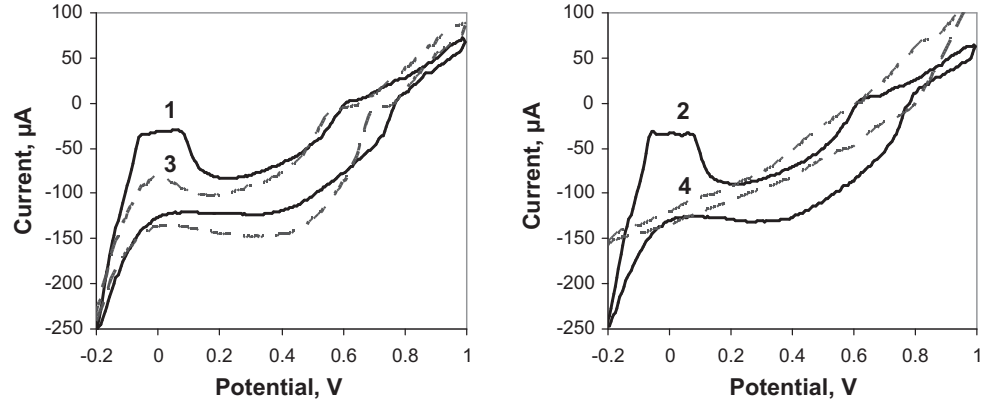

Fig. 8. CV curves of the rhodinized electrode 3 in the absence of ammonia (1) and in the presence of different concentrations of ammonia – 1 mM NH_3 (2), 3 mM NH_3 (3), 5 mM NH_3 (4).

3.3. Urea biosensor with immobilized urease on the rhodinized membrane

In order to determine the performance of urea for its application to an amperometric sensor, experiments at constant potential were performed. The presence of urea was detected through the current–time curves for electrodes prepared with the membrane 1 with 10 deposition cycles (Fig. 9). A constant potential – 0.60 V (vs. Ag/AgCl) was applied to the working electrode and the current was recorded as a function of time until a good base line was obtained. After equilibration, series of 100 μL from a 100 mM solution of urea were added to the cell with an automatic pipette and the response was recorded while the solution was stirred constantly. The ammonia was catalytically oxidized by rhodium present in the working electrode. As can be seen from Fig. 9 the current incremented linearly with the increase of the urea concentration and above 1.75 mM the amperometric response tended to a constant value. The linear dependence between the amperometric response and the urea concentration ranged from 0.1 to 1.75 mM. The linear regression equation was estimated to be $I\,(\mu A) = 1.45x + 0.32$ with a good correlation coefficient (R^2) of 0.9833 ($n = 6$). The biosensor sensitivity represented by the slope value of that regression equation (1.85 $\mu A\,mM^{-1}\,cm^{-2}$) was much higher than the biosensor sensitivities reported by other authors – 0.065 $\mu A\,mM^{-1}\,cm^{-2}$ and 0.980 $\mu A\,mM^{-1}\,cm^{-2}$ respectively [25,26]. The rhodinized membrane can provide for the efficient electron transfer between the active site of the enzyme and the electrode, thereby enhancing the urea sensing ability. The detection limit was 0.05 mM at a signal-to-

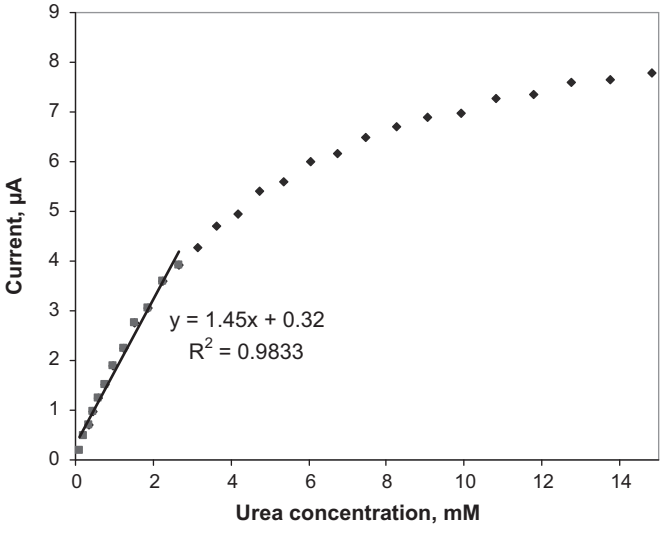

Fig. 9. Calibration curve of the amperometric urea biosensor, obtained by measuring the generated current from the successive additions of 100 μL of a 100 mM urea solution at a constant potential of 0.6 V (vs. Ag/AgCl).

Table 1
Assessment of the urease rhodinized biosensor characteristics with other previously reported amperometric urea biosensors.

Matrix	Sensitivity	Linear range	Response time	Limiting detection	Stability	Ref.
PANi-Nafion	1.81 μA (mg dl^{-1})$^{-1}$ cm^{-2}	0.006 ÷ 6 mg dl^{-1}	–	0.003 mg dl^{-1}	–	[30]
PANi-Nafion (CV regime)	5.27 μA (mg dl^{-1})$^{-1}$ cm^{-2}	3 ÷ 30 mg dl^{-1}	–	0.3 mg dl^{-1}	–	[31]
Polypyrrole	–	100 ÷ 4500 μg l^{-1}	–	60 μg l^{-1}	84 days	[32]
Polypyrrole	–	3 ÷ 15 mg l^{-1}	–	3 mg l^{-1}	28 days	[33]
Carbon paste electrode	–	2000 ÷ 3000 ppm	–	5.0×10^{-6} M	15 days	[34]
PAPCP	–	(0.16 ÷ 5.02) × 10(−5) M	40 s	0.16×10^{-5} M	60 days	[35]
Poly(vinylferrocim)	–	(0.01 ÷ 0.25) × 10(−3) M	60 s	–	29 days	[36]
Functionalized H40-Au nanoparticles	7.48×10^{-3} μA mM^{-1}	(1 ÷ 35) × 10(−3) M	3 s	1.10×10^{-5} M	126 days	[25]
Pt electrod/Hematein	0.30 μA mM^{-1} cm^{-2}	0.010 ÷ 0.200 mM	2 min	3 μM	21 days	[37]
Pt electrod/o-toluidine	0.980 μA mM^{-1} cm^{-2}	0 ÷ 0.8 mM	30 s	0.02 mM	–	[26]
Lauryl gallate	15.2 μA M^{-1} cm^{-2}	0.002 ÷ 0.750 mM	4 min	2 μM	28 days	[38]
Methylene blue	0.11 μA M^{-1} cm^{-2}	0.01 ÷ 0.25 mM	30 s	10 μM	21 days	[38]
Rhodinized polymer membrane	1.85 μA mM^{-1} cm^{-2}	0.1 ÷ 2.67 mM	15 s	50 μM	27 days	[Present work]

PANi-polyaniline, H40-hyperbranched polyester-Boltron; PAPCP-poly(N-3-aminopropyl pyrrole-co-pyrrole).

noise ratio of 3. The response to the addition of urea was immediate and stable with time for the catalysis reaching the value of the stationary current around 15 s.

The Michaelis–Menten constant K_m^{app} is an important quantity, describing enzyme affinity towards a given substrate. To examine this further K_m^{app} for urease immobilized on the prepared membrane was calculated from the Lineweaver–Burk plots using electrochemical data extracted from the calibration curves of the constructed urease biosensor (Fig. 10). The obtained K_m^{app} was 6.5 mM (correlation coefficient $R^2 = 0.9897$). K_m^{app} usually depends on the electrode material as well as the enzyme immobilization process [27]. The obtained K_m^{app} is very close to measured from us K_m of free urease – 3.2 mM and corresponded to the values reported by Krajewska [8]. The K_m^{app} of the biosensor using rhodinized membrane electrode is comparable to the results obtained by previously reported biosensors [28,29].

3.4. Reproducibility and lifetime of urea biosensor

The reproducibility of successive tests using the same biosensor was investigated. Five successive measurements using the same biosensor were carried out at a 2 mM urea solution. The relative standard deviation (R.S.D.) of the potential responses was 5.1%. The urea sensor showed a good reproducibility. It was observed that the biosensor deactivation occurred after 7 operation cycles. This disadvantage was avoided by replacing the catalytic membrane with a fresh one. The biosensor was employed for 27 days while the maximum response to urea retained 86.8%, implicating good long-term storage stability.

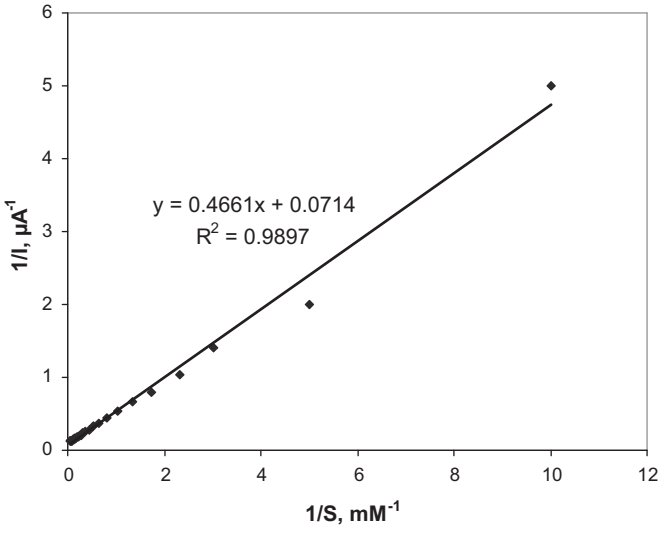

Fig. 10. Lineweaver–Burk plot from the calibration curve of the urea biosensor.

The performance of the prepared biosensor was compared to other urea biosensors [25,26,30–38] as shown in Table 1 and it is obvious that the obtained biosensor displays a very good functionality. The urea biosensor developed in this study demonstrated a linear range and a response time identical to the parameters of the urea biosensors developed by other authors.

4. Conclusions

An important advantage, as believed, of the constructed biosensor, is that the membrane carrier is a separate element and could be easily replaced after deactivation. Another advantage of the carrier is that PAN membranes possess selective and non-selective sides due to the asymmetry of the membrane pores. The enzyme molecules trapped into the pores of the non-selective membrane side cannot be washed away and are being protected from any electrochemical interference present in the solution during the measurement procedures. An important component of the prepared sensor is the electrodeposited rhodium, which insures a highly developed active surface for enzyme immobilization and electron transfer and catalyzes the electrochemical oxidation of ammonia, thus avoiding the utilization of a second enzyme.

Acknowledgements

The authors gratefully acknowledge the Bulgarian Ministry of Education and the National Science Fund and DST, India for their financial support by grants from DOO2/125 Project.

References

[1] M. Gutierrez, S. Alegret, M. Valle, Biosens. Bioelectron. 22 (2007) 2171–2178.
[2] L.M.S. Abdel, G.G. Guibault, J. Biotechnol. 14 (1990) 53–62.
[3] B. Lakard, G. Herlem, S. Lakard, A. Antoniou, B. Fahys, Biosens. Bioelectron. 19 (2004) 1641–1647.
[4] B. Krajewska, J. Mol. Catal. B: Enzym. 59 (2009) 22–40.
[5] J.H.T. Luong, P. Bouvrette, K.B. Male, Trends Biotechnol. 15 (1997) 369–377.
[6] M. Singh, N. Verma, A.K. Garg, N. Redhu, Sens. Actuators B 134 (2008) 345–351.
[7] G. Dhawan, G. Sumana, B.D. Malhotra, Biochem. Eng. J. 44 (2009) 42–52.
[8] B. Krajewska, J. Mol. Catal. B: Enzym. 59 (2009) 9–21.
[9] W. Frenzel, C.Y. Liu, Fresenius J. Anal. Chem. 342 (1992) 276–280.
[10] H. Hara, S. Matsumoto, Analyst 119 (1994) 1839–1842.
[11] S. Fan, H. Muller, B. Schweizer, W. Bohme, Fresenius J. Anal. Chem. 347 (1993) 103–106.
[12] X. Hu, N. Takenaka, S. Takasuna, M. Kitano, H. Bandow, Y. Maeda, M. Hattori, Anal. Chem. 65 (1993) 3489–3492.
[13] U. Oesch, S. Caras, J. Janata, Anal. Chem. 53 (1981) 1983–1986.
[14] Y. Miyahara, K. Tsukada, M. Miyagi, W. Simon, Sens. Actuators B 3 (1991) 287–293.
[15] F.J. Saez de Viteri, D. Diamond, Electroanalysis 6 (1994) 9–16.
[16] B.B. Rodriguez, J.A. Bolbot, I.E. Tothill, Anal. Lett. 37 (3) (2004) 415–421.

[17] B.B. Rodriguez, J.A. Bolbot, I.E. Tothill, Anal. Bioanal. Chem. 380 (2) (2004) 284–290.
[18] M. Grosman, D.G. Loffler, React. Kinet. Catal. Lett. 31 (1) (1986) 203–208.
[19] M. Cooper, MS thesis, Ohio University, 2005.
[20] B.A. Lopez de Mishima, D. Lescano, T. Molina Holgado, H.T. Mishima, Electrochim. Acta 41 (3-4) (1998) 395–404.
[21] S.P. Petrov, J. Appl. Polym. Sci. 62 (1996) 267–271.
[22] A.C.A. de Vooys, M.T.M. Koper, R.A. van Santen, J.A.R. van Veen, J. Electroanal. Chem. 506 (2) (2001) 127–133.
[23] M. Cooper, G.G. Botte, J. Electrochem. Soc. 153 (10) (2006) A1894–A1901.
[24] S. Wasmus, E.J. Vasini, M. Krausa, H.T. Mishima, W. Vielstich, Electrochim. Acta 39 (1994) 23–31.
[25] A. Tiwari, S. Aryal, S. Pilla, S. Gong, Talanta 78 (2009) 1401–1407.
[26] I. Vostiar, J. Tkac, E. Sturdik, P. Gemeiner, Bioelectrochemistry 56 (2002) 113–115.
[27] G.K. Kouassi, J. Irudayaraj, G. McCarty, J. Nanobiotechnol. 3 (2005) 1–7.
[28] J.X. Wang, X.W. Sun, A. Wei, Y. Lei, X.P. Cai, C.M. Li, Z.I. Dong, Appl. Phys. Lett. 88 (2006) 233106–233109.
[29] E. Eggenstein, M. Borchardt, C. Diekmann, B. Grundig, C. Dumschat, K. Gammann, E.M. Ekanayake, D.M. Preethichandra, K. Kaneto, Biosens. Bioelectron. 23 (2007) 107–113.
[30] W.-J. Cho, H.-J. Huang, Anal. Chem. 70 (1998) 3946–3951.
[31] Y.-C. Luo, J.-S. Do, Biosens. Bioelectron. 20 (2004) 15–23.
[32] S.B. Adeloju, S.J. Shaw, G.G. Wallace, Anal. Chim. Acta 341 (1997) 155–160.
[33] S.B. Adeloju, S.J. Shaw, G.G. Wallace, Anal. Chim. Acta 323 (1996) 107–113.
[34] J.H. Jin, S.H. Paek, C.W. Lee, N.K. Min, S.I. Hong, J. Korean Phys. Soc. 42 (2003) S735–S738.
[35] B.V. Rajesh, W. Takashima, K. Kaneto, Biomaterials 26 (2005) 3683–3690.
[36] F. Kuralay, H. Ozyoruk, A. Yildiz, Sens. Actuators B: Chem. 114 (2006) 500–507.
[37] A. Pizzriello, M. Stredansky, S. Stredanska, S. Miertus, Talanta 54 (2001) 763–772.
[38] M. Stred'ansky, A. Pizzariello, S. Stred'anska, S. Miertus, Anal. Chim. Acta 415 (2000) 151–157.